

## **"FOLLOW-THE-LEADER" CONTROL FOR A TRAIN-LIKE-VEHICLE. IMPLEMENTATION AND EX- PERIMENTAL RESULTS.**

A.Micaelli <sup>†</sup>, F.Louveau <sup>†</sup>, D.Sabourin <sup>†</sup>,  
C.Canudas de Wit <sup>‡</sup>, A-D.Ndoudi-Likoho <sup>‡</sup>

<sup>†</sup> Commissariat à l'Energie Atomique (CEA) Section de Téléopération  
et de Robotique, 92265 Fontenay-aux-Roses, France.

Email: micaelli@suisse.far.cea.fr

<sup>‡</sup> Laboratoire d'Automatique de Grenoble (LAG), 38402 Saint-Martin  
d'Hères, France.

Email: canudas@lag.grenet.fr

### **Abstract**

*This paper presents some practical implementation aspects and results of a particular control law dedicated to Train-Like-Vehicles (TLV) for trajectory tracking purpose. The CEA's demonstrator consists of two modules. This is a partial but representative mockup of a future 4-modules vehicle devoted to maintenance and intervention in nuclear plants, and which is now on development within the frame of the Teleman (MESSINA) project.*

## **1 Introduction**

In order to face the issue of heavy duty applications in clustered indoor environments, and more specifically, intervention and maintenance in nuclear power plants, a multibody Train-Like-Vehicle concept has been proposed in the recent past years. Besides the fact that the payload volume of such a vehicle is proportional to the number of its carts, the increase of complexity induced by adding a new cart will never reach the complexity entailed by adding another autonomous vehicle.

Among all the possible motions for such multibody systems, the "Follow the Leader" behaviour is considered as being the most relevant. The leading cart (first in the motion direction) is controlled in teleoperation mode. The following carts must track, as accurately as possible, the path travelled by the leading cart. The resulting surface swept by the whole vehicle will then be close to the surface swept by the first cart. Moreover, thanks to a vertical translation placed between each couple of modules, the vehicle can move on slopes while all the modules stay vertical. This last aspect is not addressed in the present paper.

In [1], the theoretical bases of the control law have been established. In this paper, after recalling the main principles of the control, we describe all the peculiar choices we made in order to provide the robot with a good behaviour. The first part is concerned with the reference trajectory and its on line computation. In the second part, a special attention

is paid to the robot's reference configuration. The third part explains how the control parameters are tuned while the fourth one is devoted to the control limitations. Finally, experimental and successful results of a real implementation on a TLV mockup are given and discussed.

## 2 Theoretical bases

For a more detailed theoretical presentation, the reader is invited to refer to [1].

### 2.1 Modelling

The TLV here considered consists of a series of  $n$  "unicycle-type" carts linked together by a rod of length  $l$ . The articulation between two rods is a free rotation whose axis is vertical and identical to the undercarriage steering axis. Fig.1 presents the configuration variables  $\alpha_i, \beta_i$  where  $i$  is the module number (the first module is number 0 but no couple  $(\alpha, \beta)$  can be defined for this module).

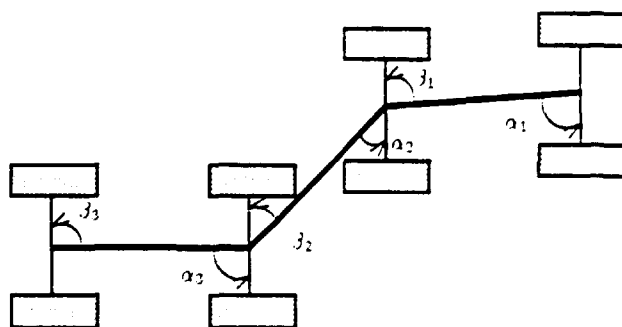


Figure 1: Schematic description of the TLV

If only two modules of the TLV are considered (for example the two first ones), the following state equations can be derived :

$$\begin{cases} \dot{x}_0 = v_0 \cos \theta \\ \dot{y}_0 = v_0 \sin \theta \\ \dot{\alpha} = -\frac{v_0}{l} \frac{\sin(\alpha - \beta)}{\sin \beta} + w_2 \\ \dot{\beta} = -\frac{v_0}{l} \frac{\sin(\alpha - \beta)}{\sin \beta} + w_1 \end{cases} \quad \text{if } \sin \beta \neq 0 \quad (1)$$

where :

- $(\dot{x}_0, \dot{y}_0)$  represents the velocity coordinates of module 0 relative to a fixed frame, and projected onto a mobile frame linked to the rod;
- $\theta$  is the orientation of the first module;
- $v_0$  : the curvilinear velocity of module 0;

- $w_0$  et  $w_1$  express the rotation velocities of modules 0 and 1 respectively relative to a fixed frame.

The singularity  $\sin\beta = 0$  stems from an existing relation between the modules curvilinear velocities. In order to deal with this problem, we introduced  $\sin\beta$  as a factor in  $v_0$  ( $v_0 = v\sin\beta$ ). Moreover, as the set of all possible trajectories for such a vehicle exceeds the actual need, the reference trajectory is constrained so that  $\sin\alpha$  and  $\sin\beta$  do not reach 0. This condition can be easily satisfied if  $\vec{l}_0 \cdot \vec{l}_1 > 0$  (See Fig.2).

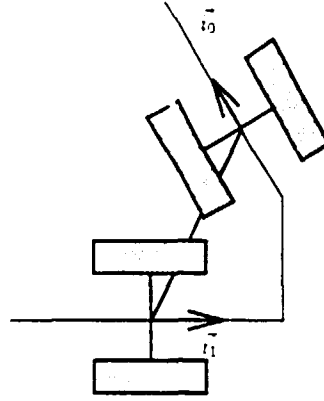


Figure 2: Example of a forbidden trajectory

In addition, the control laws are designed so as to satisfy the following conditions :

$$\begin{cases} \sin\alpha_i > 0 \\ \sin\beta_i > 0 \end{cases} \quad \forall i \in [1, n-1] \quad (2)$$

Consequently, all the modules move in the same direction, and for the sake of legibility, only one forward direction is here considered. In case of backward movements, the first module is replaced by the last one and this does not modify the approach presented below. As far as we are concerned,  $w_0$  is set according to a desired path and with respect to (2). The remaining degree of freedom, for the control design, consists of  $w_1$  which is tuned so that the second module follows the first one. Limiting the presentation to a two-modules system does not make it less generic as shown in [1].

## 2.2 Reference model

The control law presented in [1] is designed so as to cancel a sort of distance between the actual system and the reference one. This reference system is parametrized by  $(\alpha, \beta)$ -type variables and can be written as :

$$\begin{cases} \dot{\alpha}_r = -\frac{v_0}{l} \frac{\sin(\alpha_r - \beta_r)}{\sin\beta_r} + w_0 \\ \dot{\beta}_r = -\frac{v_0}{l} \frac{\sin(\alpha_r - \beta_r)}{\sin\beta_r} + w_{1r} \end{cases} \quad (3)$$

where :

- $(\alpha_r, \beta_r)$  define the configuration of the reference robot;
- $w_1$  is the theoretical steering velocity of the second reference module.

### 2.3 Control law

Combining the two last equations of systems (1) and (3) yields the following system :

$$\begin{cases} \frac{\dot{\alpha} - \dot{\alpha}_r}{\beta - \beta_r} = \frac{v_r}{l} \left[ -\frac{\sin(\alpha - \beta)}{\sin \beta} + \frac{\sin(\alpha_r - \beta_r)}{\sin \beta_r} \right] \\ \frac{\dot{\beta} - \dot{\beta}_r}{\beta - \beta_r} = \frac{v_r}{l} \left[ -\frac{\sin(\alpha - \beta)}{\sin \beta} + \frac{\sin(\alpha_r - \beta_r)}{\sin \beta_r} \right] + w_3 \end{cases} \quad (4)$$

where  $w_3 = w_1 - w_{1r}$ .

In order to build up an error system and to make easier the construction of a Lyapunov function, an intermediate variable :

$$\beta_d = \text{atan2} \left[ \sin \alpha, k_\alpha(\alpha - \alpha_r) + \sin \alpha_r \frac{\cos \beta_r}{\sin \beta_r} \right] \quad (5)$$

must be introduced, leading to the following system :

$$\begin{cases} \dot{\tilde{\alpha}} = \frac{v_r}{l} \left\{ \left[ \frac{\cos \alpha - \cos \alpha_r}{\alpha - \alpha_r} - k_\beta \right] \tilde{\alpha} + \frac{\lambda}{\sin \beta} \sin \tilde{\beta} \right\} \\ \dot{\tilde{\beta}} = \frac{v_r}{l} \left\{ \left[ \frac{\cos \alpha - \cos \alpha_r}{\alpha - \alpha_r} - k_\alpha \right] \tilde{\alpha} + \frac{\lambda}{\sin \beta} \sin \tilde{\beta} \right\} - \dot{\beta}_d + \dot{\beta}_r + w_3 \end{cases} \quad (6)$$

with  $\tilde{\alpha} = \alpha - \alpha_r$ ,  $\tilde{\beta} = \beta - \beta_d$ , and :

$$\lambda = \sqrt{\sin^2 \alpha + \left[ k_\alpha(\alpha - \alpha_r) + \sin \alpha_r \frac{\cos \beta_r}{\sin \beta_r} \right]^2} \quad (7)$$

**Remark**  $\beta_d$  given by (5) may not be well-defined when  $\sin \alpha$  is close to 0. Practically, the problem was solved by replacing (5) with a slightly different formula which makes tend  $\beta_d$  to  $\beta_r$  when  $\sin \alpha$  tends to 0.

Choosing the Lyapunov function as :

$$V = \frac{1}{2} \left[ \tilde{\alpha}^2 + \frac{1}{\lambda_\beta} \tilde{\beta}^2 \right] \quad \text{with} \quad \lambda_\beta > 0 \quad (8)$$

it can be shown that the control :

$$w_1 = -\lambda_\beta \frac{v}{l} \lambda \tilde{\alpha} \frac{\sin \tilde{\beta}}{\tilde{\beta}} - \dot{\alpha} + w_r + \dot{\beta}_d - k_\beta \tilde{\beta}, k_\beta \geq 0 \quad (9)$$

gives :

$$\dot{V} \leq 0$$

Under some initial conditions and some constraints on the reference trajectory, it can be proved that the convergence is ensured. The only difficulty stems from the demonstration that  $\sin \beta$  does not converge toward 0. Of course, we must have  $\sin \beta_r \geq \epsilon_{\beta_r} > 0$ .

### 3 Reference trajectory

As our vehicle is destined to be mainly teleoperated, the trajectory of the first module is a priori unknown. Therefore, we chose to store the position of the first module at a fixed and rather small step (practically, 5mm was adequate). Then, this stored trajectory must be smoothly interpolated, because the control law contains some derivatives of the stored reference. As the stored points are close together, a simple approximation is calculated on a moving window. Typically, a 10cm long window was chosen according to the desired accuracy. An illustration of our filter is given by Fig.3.

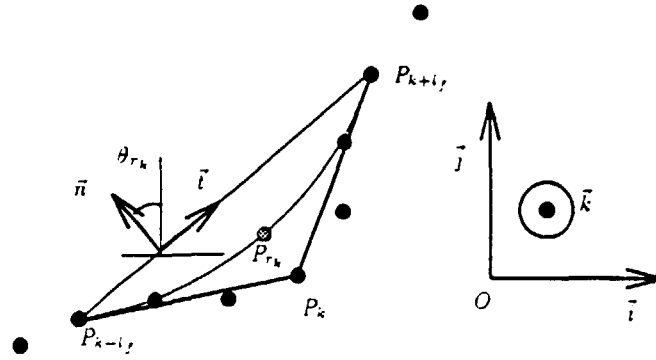


Figure 3: Interpolation of the stored trajectory

In Fig.3, the window is 6 interval long ( $l_f = 3$ ), and the different variables are defined as follows :

- $P_k$  : the stored points;
- $P_{r_k}$  : the point obtained after filtering;
- $\theta_{r_k}$  : the filtered tangent orientation at  $P_{r_k}$ ;
- $c_{r_k}$  : the filtered estimated curvature at  $P_{r_k}$ .

Among all possible filters that could have been applied, our filter is simple, in terms of calculations, and efficient enough.

A last but not least aspect of this reference trajectory is concerned with the maximum curvilinear velocity which is attached to each reference point. Indeed, this velocity must be lowered first relative to the curvature  $c_{r_k}$  and the maximum allowable steering velocity  $w_{max}$ , and then relative to the maximum curvilinear velocity attached to the next point in order to satisfy a maximum acceleration constraint  $\gamma_{max}$ . The next equation deals with the first limitation :

$$v_{r_k} = \min \left( v_{max}, \frac{w_{max}}{|c_{r_k}|} \right)$$

The second constraint is taken into account by backpropagating the following expression :

$$v_{r_{k-1}} = \min \left( v_{r_{k-1}}, \sqrt{2\gamma_{max} \|P_{r_k} - P_{r_{k-1}}\| + v_{r_k}^2} \right)$$

until it does not affect the considered velocity any longer. In other simpler words, this constraint means that the velocity must be reduced before a sharp turn.

## 4 The reference configuration

In order to compute the reference robot configuration, a point corresponding at best to an ideal position of the second module must be found out of the stored positions. As the first and second modules move in the same direction - i.e. forward - according to paragraph 2.1, the stored points are examined one by one in only one and forward direction.

Once the best point is found, an interpolation must be performed in order to avoid discontinuities which could affect the control, especially in case of sharp turns. Because of the small steps between two successive stored points, a simple linear interpolation has been chosen.

Now, the procedure we applied is detailed. Considering the theory, the best solution is given by a circular projection of the second module onto the reference trajectory. According to Fig.4, the search must stop as soon as  $\| M_0 \overline{P_{r_{k+1}}} \| \leq l$ .

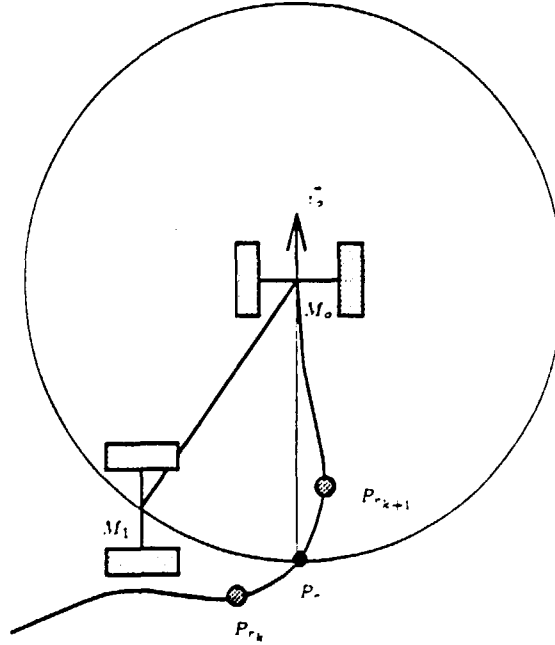


Figure 4: Case where  $\| M_0 \overline{P_{r_k}} \| > l$  and  $\| M_0 \overline{P_{r_{k+1}}} \| < l$

Then, the linear interpolation is characterized by the ratio  $r = \frac{\| P_r \overline{P_{r_{k+1}}} \|}{\| P_r \overline{P_{r_{k+1}}} \|}$ .

As this value is not directly available, it can be approximated by :

$$r = \frac{\| \overline{M_2 P_{r_{k+1}}} \| (l - \| \overline{M_2 P_{r_{k+1}}} \|)}{\| \overline{M_2 P_{r_{k+1}}} \cdot \overline{P_{r_k} P_{r_{k+1}}} \|}$$

Unfortunately, a circular projection may bring some drawbacks, especially in case of sharp turns (even if the turn angles does not exceed  $90^\circ$ ). Such difficulty is illustrated by Fig.5.

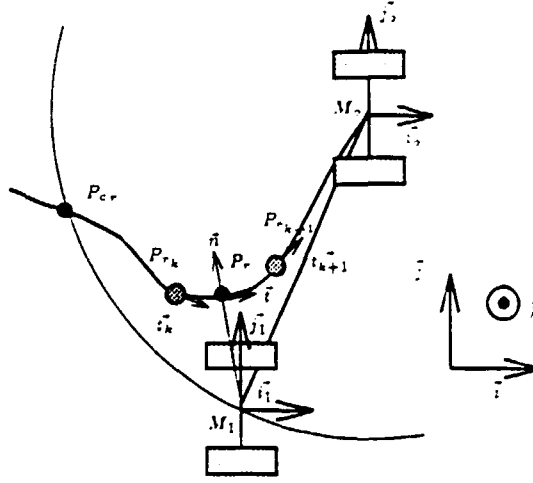


Figure 5: Case where  $\| \overline{M_2 P_{r_k}} \| < l$  and  $\| \overline{M_2 P_{r_{k+1}}} \| < l$

A circular projection would give a point  $P_{cr}$  which is much behind the second module relative to the reference trajectory, and far from the turn as the second module is very close to it. Considering that the second module velocity is constrained by the maximum velocities attached to points  $P_{r_k}$  and  $P_{r_{k+1}}$ , a severe overshooting may occur.

In order to solve this problem, it is worth replacing the circular projection by an orthogonal one in such situations.  $r$  can be then approximated by :

$$r = \frac{\| \overline{M_1 P_{r_{k+1}}} \cdot \overline{P_{r_k} P_{r_{k+1}}} \|}{\| \overline{P_{r_k} P_{r_{k+1}}} \|^2}$$

Of course, this projection does not quite correspond to the theory explained in section 2, but, practically, this little spin applied to the theory does not appear to be significant. For the sake of exactness, other methods like these proposed in [2] and [3] would be preferred.

## 5 Tuning the control parameters

In the case where  $k_\beta = \frac{\nu_0}{t} k'_\beta$  with  $k'_\beta > 0$ , the error system (6) can be locally approximated as :

$$\begin{cases} \frac{d\tilde{\alpha}}{d\nu} = \frac{1}{t} \left[ -k'_\alpha \tilde{\alpha} + \frac{\sin \alpha_r}{\sin^2 \beta_r} \tilde{\beta} \right] \\ \frac{d\tilde{\beta}}{d\nu} = \frac{1}{t} \left[ -\frac{\lambda_2 \sin \alpha_r}{\sin^2 \beta_r} \tilde{\alpha} - k'_\beta \tilde{\beta} \right] \end{cases} \quad (10)$$

where  $\nu = \int_0^t v_o(\tau) d\tau$  replaces the independent variable  $t$ .

If  $\frac{\lambda_2 \sin^2 \alpha_r}{\sin^4 \beta_r}$  is supposed to be much smaller than  $k'_\alpha k'_\beta$  ( $k'_\alpha = k_\alpha - \sin \alpha_r$ ) and, if  $\sin \beta_r$  and  $\sin \alpha_r$  are slowly varying, then choosing  $\zeta = 1$  and  $\omega$  as the damping factor and the desired natural frequency (rad/s) respectively, yields the following expressions for  $k'_\alpha$  and  $k'_\beta$  :

$$k'_\alpha = k'_\beta = t\omega \quad (11)$$

It could be worthwhile that  $\tilde{\beta}$  converges toward 0 even if  $v_o = 0$ . This can be done by adding a small constant to  $k_\beta$  ( $k_\beta = \frac{\nu_0}{t} k'_{\beta_1} + k'_{\beta_2}$ ).

For our robot, we chose :

$$\begin{cases} k_\alpha = 10 \\ k_\beta = 10\nu_0 + 1 \end{cases} \quad (12)$$

## 6 Control Saturation

### 6.1 Limiting the curvilinear velocity

The theory presented in section 2 does not take into account the actuators saturations. These limitations can easily lead to instability. Noting that the control law (9) can be written as :

$$w_1 = av_o + b$$

with  $b$  quite small (introduced by  $k'_{\beta_2}$ ), we propose to lower  $v_o$  by the following factor :

$$\mu = \min \left( 1, \frac{w_{max} - b \operatorname{sign}(w_1)}{|av_o| + \epsilon} \right) \quad , \quad \epsilon > 0 \quad \text{and small} \quad (13)$$

### 6.2 Taking into account the joints limitations

Generalizing the constraints (2),  $\alpha$  and  $\beta$  must belong to the intervals  $[\alpha_{inf}, \alpha_{sup}]$  and  $[\beta_{inf}, \beta_{sup}]$  respectively.  $\alpha$  and  $\beta$  will remain included in these intervals as long as the controls  $w_o$  and  $w_1$  belong to the intervals  $[w_{oinf}, w_{osup}]$  and  $[w_{1inf}, w_{1sup}]$  respectively with :

$$\begin{cases} w_{oinf} = \max \left[ \sqrt{2\Gamma_{max} |\alpha_{inf} - \alpha| \operatorname{sign}(\alpha_{inf} - \alpha)}, -w_{max} \right] \\ w_{osup} = \min \left[ \sqrt{2\Gamma_{max} |\alpha_{sup} - \alpha| \operatorname{sign}(\alpha_{sup} - \alpha)}, w_{max} \right] \end{cases}$$



and :

$$\begin{cases} w_{inf} = \max \left[ \sqrt{2\Gamma_{max}|\beta_{inf} - \beta|} \text{sign}(\beta_{inf} - \beta), -w_{max} \right] \\ w_{sup} = \min \left[ \sqrt{2\Gamma_{max}|\beta_{sup} - \beta|} \text{sign}(\beta_{sup} - \beta), w_{max} \right] \end{cases}$$

where  $\Gamma_{max}$  is the maximum allowable steering acceleration.

## 7 Experimental results

The control scheme presented above has been first validated on the *TLV* simulator taking into account all the limitations of the real system (maximum velocities and accelerations, sampling rate....). After this validation phase, the same controller has been applied to a 2-modules mockup at CEA. All the algorithms are implemented on a *TMS320C30* computer from TEXAS and take a little less than *2ms* in a *5ms* sample period. The tests were carried out on almost forbidden trajectories so that the vehicle was forced to move very close to singular points ( $\sin\beta_r = 0$ ). On Fig.6, such a trajectory is plotted. The solid line reflects the filtered trajectory tracked by the first module while the dashdot line represents the trajectory of the second one.

Globally, a good behaviour of the robot is obtained. Around almost singular points, the second module deviates slightly from the desired path and a small error occurs which does not exceed *2.5cm* (See Fig.7).

This result is quite acceptable according to the Telemat/MESSINA specifications. On Fig.8, the different velocities  $v_o$ ,  $w_o$  and  $w_1$  are drawn, and it can be noted that the velocities limitations are reached most of the time without giving rise to any instability.

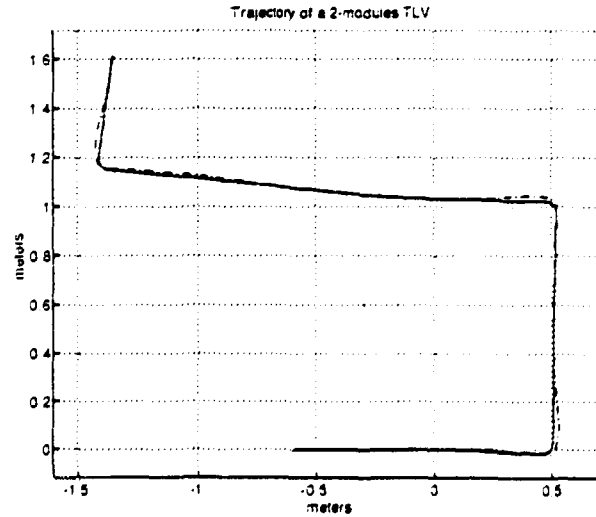


Figure 6: Trajectory of the two-modules *TLV*

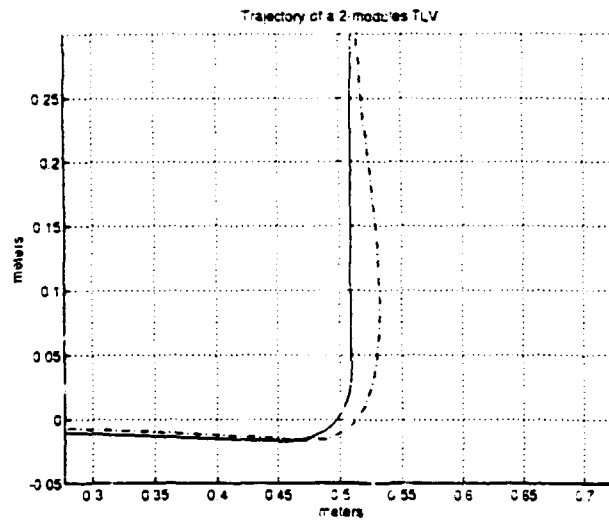


Figure 7: After a sharp turn

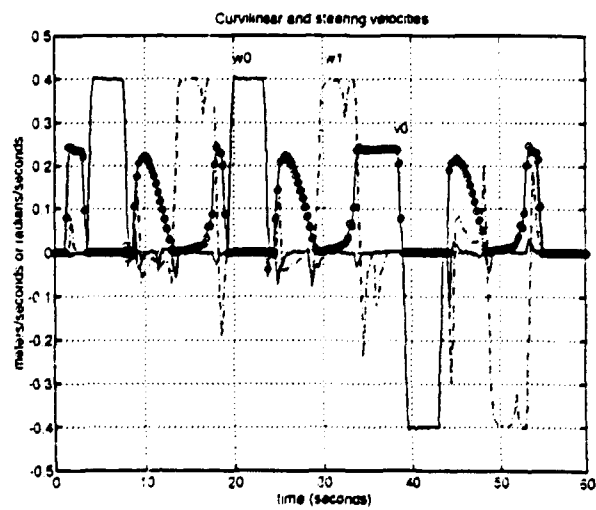


Figure 8: Velocities diagram

On the next two figures ( Fig.9 and Fig.10), a more complex trajectory and its related velocities diagram are plotted.

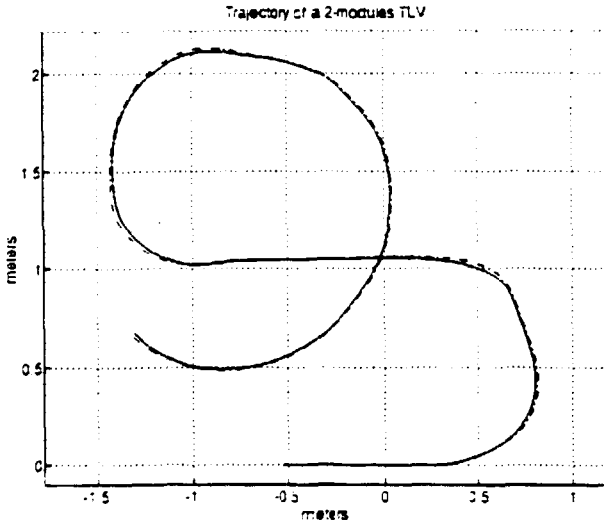


Figure 9: Complex trajectory of the two-modules *TLV*

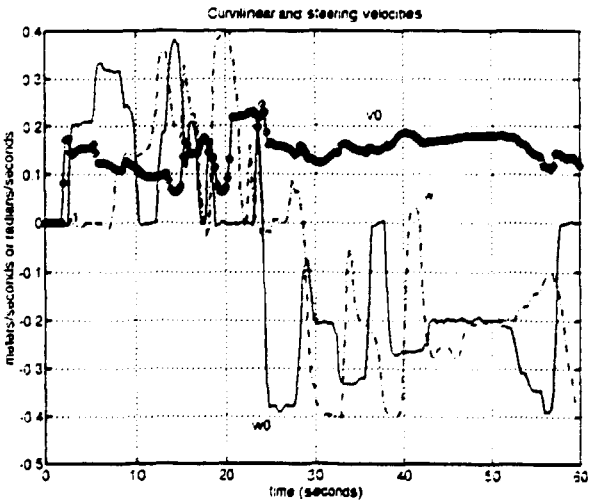


Figure 10: Velocities diagram

## 8 Conclusion

At this stage, the control presented in [1] is efficient and a good behaviour of the real robot is obtained provided a great care is given to all the problems which rarely occur in an ideal simulation environment. As said above, other non-linear control laws like [2] and [3] could be applied to solve the "Follow-the-leader" problem and it would be interesting to make some comparisons. However, the difficult situations ( $\sin \beta$  small) will not be canceled although they appear in a different way. Now, if there is a real need to make such a robot more accurate in sharp turns, other approaches based on rules, for example, could be investigated. Nevertheless, one of the most attractive aspects of the present control scheme is that one and only one algorithm gives a satisfactory solution for all the permitted situations that our *TLV* will meet.

## References

- [1] C.Canudas de Wit, A-D.Ndoudi-Likoho,A.Micaelli, "*Feedback Control for a Train-Like-Vehicle*", IEEE Internatinal Conference on Robotics and Automation, San Diego, May 1994.
- [2] C.Samson, "*Path Following and Time-varying Stabilization of a Wheeled Mobile Robot*", Proc. Int. Conf. ICARCV'92, RO-13.1, Singapore, September 1992.
- [3] A.Micaelli, C.Samson, "*Trajectory Tracking for Unicycle-Type and Two-Steering-Wheels Mobile Robots*", INRIA Report No.2097, Sophia-Antipolis, Novembre 1993.

Copie :

M. JM. DETRICHE  
M. H. CHAMEAUD  
M. F. LOUVEAU  
M. DI. SABOURIN